https://doi.org/10.20965/jdr.2013.p0878

Paper:

A New Ground Motion Prediction Equation for Japan Applicable up to M9 Mega-Earthquake

Nobuyuki Morikawa and Hiroyuki Fujiwara

National Research Institute for Earth Science and Disaster Prevention
Tennodai 3-1, Tsukuba, Ibaraki 305-0006, Japan
E-mail: morikawa@bosai.go.jp

[Received May 1, 2013; accepted July 31, 2013]

In this study we suggest a new ground motion prediction equation applicable up to the moment magnitude 9 using the strong motion records from the 2011 Tohoku-oki earthquake. We determined a base model with moment magnitude and the shortest distance from the source fault as parameters. In order to avoid overestimating amplitude at magnitude larger than 8, we examined two models – a quadratic magnitude term and a linear magnitude term with a complete amplitude saturation term at some Mw. We then adopt additional correction terms corresponding to amplification by deep sediments or shallow soft soils, and anomalous seismic intensity distribution in order to improve prediction.

Keywords: ground motion prediction equation, the 2011 Tohoku-oki earthquake, seismic hazard assessment

1. Introduction

The ground motion prediction equation (GMPE) based on actually observed records is a useful tools in seismic hazard assessments. The equation for peak ground velocity (PGV) by Si and Midorikawa (1999) [1], for instance, is used in assessing national seismic hazard maps for Japan published by the Headquarters for Earthquake Research Promotion of Japan. The applicability of existing GMPEs for earthquakes of magnitude 9 is not valid, however, because strong-motion records of such earthquakes were not obtained. The Tohoku-oki earthquake (moment magnitude (Mw) = 9.0) on March 11, 2011, was the largest event recorded by dense strong-motion observation networks in Japan. In this paper, we suggest a new GMPE for Japan directly applicable up to Mw9 using strong-motion records.

2. Data

We updated the strong-motion database of Kanno et al. [2] by adding the strong-motion records up to the end of 2011. We collected waveform data from the National Research Institute for Earth Science and Disaster Prevention (NIED; K-NET and KiK-net), the Japan Meteorological Agency (JMA) and the Port and Airport Research Institute (PARI). We used Mw determined by F-net, NIED, for added records. We also collected the source fault models listed in **Table 1** in order to calculate source distance.

We selected data from the database for regression analysis using the following criteria:

(1) Mw is larger than or equal to 5.5.

(2) Data were recorded on the ground surface.

(3) Two orthogonal horizontal components are available.

(4) At least 5 stations were triggered by the event.

(5) The source distance is shorter than 200 km.

(6) Data truncated at a source distance that predicted PGA by Kanno et al. [2] were smaller than 10 cm/s/s.

In this study, we use the shortest distance from source faults to observed stations (X in km). The magnitude-distance distribution of strong-motion data used in this regression analysis is shown in **Fig. 1**. Target strong-motion parameters are JMA seismic intensity (INT), peak ground acceleration (PGA in cm/s/s), peak ground velocity (PGV in cm/s) and 5% damped acceleration spectra (SA in cm/s/s). The peak value is the peak square root of the sum of squares of two orthogonal horizontal components in the time domain. SA consist of 47 periods between 0.05 and 10 seconds. The number of earthquakes was 333 and strong-motion records was 21,681.

3. Base Model

We first obtained a simple model with only Mw and X as the parameters, i.e., the base model. The weighting scheme has no physical meaning but is useful for increasing the statistical power of near-source data. In regression analysis, we apply the following weighting scheme:

$$weight = \begin{cases} 8.0 & X \leq 10 \text{ km} \\ 4.0 & 10 \text{ km} < X \leq 20 \text{ km} \\ 2.0 & 20 \text{ km} < X \leq 40 \text{ km} \\ 1.0 & 40 \text{ km} < X \end{cases} \quad \cdots \quad (1)$$

In this study, we obtain regression coefficients individually for each earthquake type – I: crustal, II: subduction plate-boundary, and III: subduction intra-plate – to see

Table 1. Events of fault plane models added to our database. The hypocenter location is after the JMA.

Origin time [JST]	Mw	Lat. [N]	Lon. [E]	Dep. [km]	Type	Ref.
2004/09/05 19:07	7.2	33.03	136.80	38	III	[3]
2004/09/05 23:57	7.4	33.14	137.14	44	III	[3]
2004/09/07 08:29	6.5	33.21	137.29	41	III	[3]
2004/10/23 17:56	6.5	37.29	138.87	13	I	[4]
2004/10/23 18:11	5.7	37.25	138.83	12	I	[4]
2004/10/23 18:34	6.2	37.31	138.93	14	I	[4]
2004/10/27 10:40	5.8	37.29	139.03	12	I	[5]
2004/11/08 11:15	5.5	37.40	139.03	0	I	[5]
2004/11/29 03:32	7.0	42.95	145.28	48	II	[3]
2004/12/06 23:15	6.7	42.85	145.34	46	II	[3]
2005/03/20 10:53	6.5	33.74	130.18	9	I	[6]
2005/08/16 11:46	7.1	38.15	142.28	42	II	[7]
2007/03/25 09:41	6.7	37.22	136.69	11	I	[7]
2007/07/16 10:13	6.6	37.56	138.61	17	I	[8]
2008/05/08 01:02	6.2	36.23	141.95	60	II	[9]
2008/05/08 01:45	6.8	36.23	141.61	51	II	[9]
2008/06/14 08:43	6.9	39.03	140.88	8	I	[10]
2008/07/19 11:39	6.9	37.52	142.26	32	II	[9]
2008/07/24 00:26	6.8	39.73	141.64	108	III	[11]
2008/09/11 09:20	6.8	41.78	144.15	31	II	[9]
2009/08/11 05:07	6.2	34.79	138.50	23	III	[12]
2011/03/09 11:45	7.2	38.33	143.28	8	II	[13]
2011/03/11 14:46	9.0	35.60	141.50	24	II	[14]
2011/03/11 15:08	7.4	39.84	142.78	32	II	[13]
2011/03/11 15:15	7.8	36.11	141.27	43	II	[13]
2011/03/12 03:59	6.2	36.99	138.60	8	I	[13]
2011/03/15 22:31	5.9	35.31	138.71	14	I	[13]
2011/03/19 18:56	5.8	36.78	140.57	5	I	[13]
2011/04/07 23:32	7.1	38.20	141.92	66	III	[13]
2011/04/11 17:16	6.6	36.95	140.67	6	I	[13]
2011/04/12 14:07	5.8	37.05	140.64	15	I	[13]
2011/06/23 06:50	6.6	39.95	142.59	36	II	[13]
2011/07/10 09:57	7.0	38.03	143.51	34	III	[13]
2011/07/23 13:34	6.3	38.87	142.09	47	II	[13]
2011/07/25 03:51	6.2	37.71	141.63	46	II	[13]
2011/07/31 03:53	6.3	36.90	141.22	57	III	[13]
2011/08/01 23:58	5.8	34.71	138.55	23	III	[13]
2011/08/19 14:36	6.3	37.65	141.80	51	III	[13]
2011/09/17 04:26	6.6	40.26	143.09	7	II	[13]
2011/11/24 19:25	6.1	41.75	142.89	43	II	[13]

Type: I = crustal, II = subduction plate-boundary, III = subduction intra-plate Ref: Referred fault model

differences in source or path characteristics among the three types. In order to examine the modeling of a magnitude term, we first assume the following simple model:

$$\log pre_{ij} = \alpha_i + b_{ij\_k} \cdot X_{ij} - \log X_{ij} \quad . \quad . \quad . \quad . \quad . \quad (2)$$

where pre_{ij} is the predicted PGA, PGV or SA for earthquake i at station j, and k is the suffix of the earthquake type. Note that log *pre* changes to *pre*/2 in the case of JMA seismic intensity considering its definition. We used

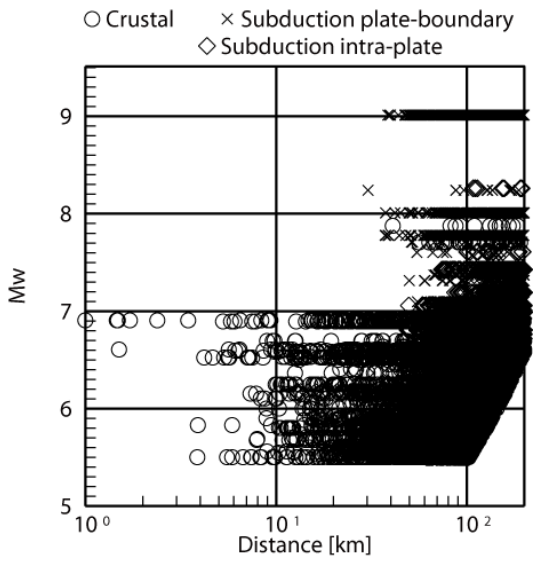

Fig. 1. Magnitude-distance distribution of strong-motion records used in regression analysis.

a base 10 logarithm throughout this study. The coefficient α_i was obtained for each earthquake. The relationship between Mw and the α_i obtained is shown in **Fig. 2**. The value of α_i for an Mw9 earthquake is similar to that for an Mw8 plate-boundary earthquake. This implies that amplitude saturates at Mw larger than about 8 and further, that strong-motion amplitudes saturate at larger Mw. We examined two models to express saturation. Model 1 is expressed with a quadratic magnitude term:

$$\log pre = a_1(Mw'_1 - Mw_1)^2 + b_{1\_k}X + c_{1\_k} - \log(X + d_1 \cdot 10^{e_1 Mw'_1}) \pm \sigma_1 \quad . \quad (3)$$

$$Mw'_1 = \min(Mw, Mw_{01}) \quad . \quad . \quad . \quad . \quad . \quad . \quad . \quad . \quad (4)$$

where a_1, b_{1_k}, c_{1_k}, d_1 and e_1 are regression coefficients, and σ_1 is standard deviation. Mw_{01} is the moment magnitude at which amplitude is saturated.

This type of model was proposed already in order to express the amplitude saturation at a large magnitude that was predicted from the scaling law of the source spectrum [15]. Because the value of α_i for earthquakes of Mw9 is similar to that of Mw8 from **Fig. 2**, however, we adopt complete amplitude saturation at certain magnitude Mw_{01}.

Model 2 is expressed with a linear magnitude term with complete amplitude saturation at Mw_{02}:

$$\log pre = a_2 Mw'_2 + b_{2\_k}X + c_{2\_k} - \log(X + d_2 \cdot 10^{e_2 Mw'_2}) \pm \sigma_2 \quad . \quad . \quad . \quad (5)$$

$$Mw'_2 = \min(Mw, Mw_{02}) \quad . \quad . \quad . \quad . \quad . \quad . \quad . \quad . \quad (6)$$

where a_2, b_{2_k}, c_{2_k}, d_2, e_2 are regression coefficients and σ_2 is standard deviation. Since there are few records of mega-earthquakes or near source region sites, we assume here that Mw_0, Mw_1 and e take a constant value independent of both earthquake type (I, II and III) and strong-motion parameter (period). We also assume that coefficient a is independent of earthquake type [1]. We fixed

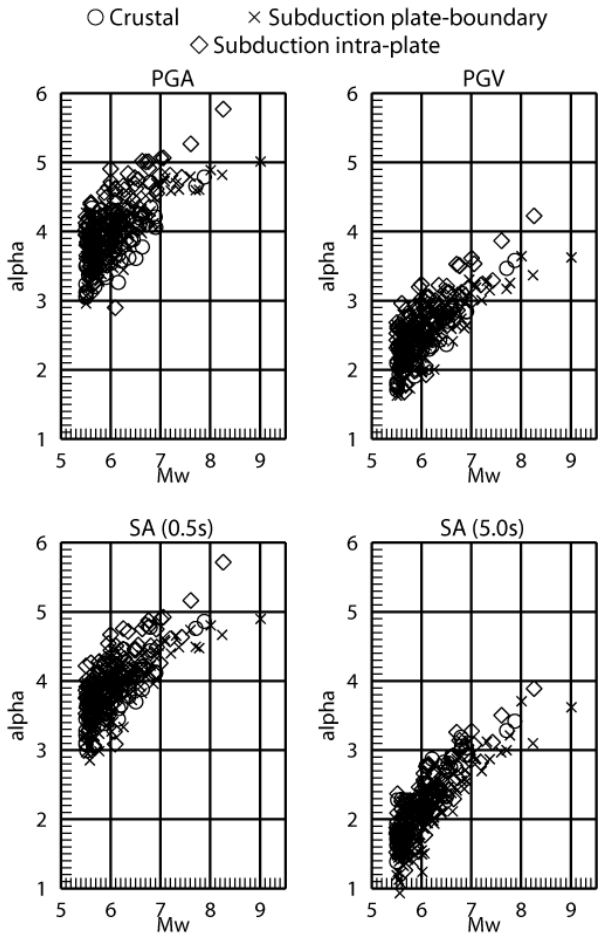

Fig. 2. Example of relationship between coefficient α and moment magnitude (Mw).

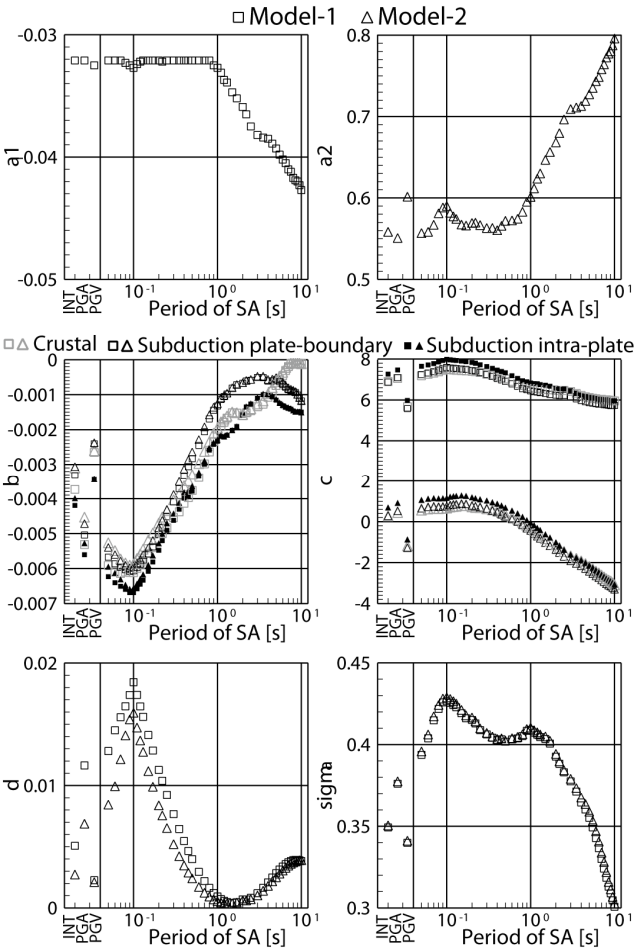

Fig. 3. Obtained regression coefficients and standard deviations.

the value of e_1 and e_2 at 0.5 referencing past studies. We used two-step stratified regression analysis method [16] and applied an iterative procedure [17]. We first obtained $Mw_{01} = 8.2$, $Mw_1 = 16.0$ and $Mw_{02} = 8.1$ by changing Mw_0 in units of 0.1 and Mw_1 in units of 1. For SA, we performed smoothing for the period in order to avoid unnatural unevenness. The coefficients obtained are shown in **Fig. 3** and Appendix 1. The standard deviation of Model 1 is slightly lower than that of model 2. This difference is not statistically significant, however, so we could not conclude which model was better.

4. Addistional Correction Terms

We examined additional correction terms to improve the accuracy of prediction results. We used residual data between the observed amplitude and the predicted one calculated from the base model. Strictly speaking, residual data from model 1 differed from data from model 2, but we used only the residual data from model 1 in this analysis.

4.1. Amplification by Deep Sedimentary Layers

To examine amplification by deep sedimentary layers, we extracted data from all data used in the above regression analysis using the following criteria:

(a) Focal depth is shallower than 30 km.

(b) Observed peak ground acceleration is smaller than 100 cm/s/s.

(a) was to avoid the anomalous seismic intensity distribution mentioned in section 4.3 and (b) was to avoid nonlinear site responses.

Fujiwara et al. [18] constructed an underground structure model of deep sedimentary layers for all of Japan. Their model mainly consists of 6 layers whose S-wave velocity (Vs) is 600, 1100, 1400, 1700, 2100, or 2700 m/s on seismic bedrock whose Vs is 3100 m/s or more. Because there are quite a few sites in the basin area where the seismic velocity profile up to seismic bedrock is available, we used this underground structure model in this study. **Fig. 4** shows an example in which relationship between the residual and depth to each layer at the site. We saw that the residual tends to become larger so that the top depth to the layer becomes deep. We modeled this trend as follows:

$$G_d(=\log[obs/pre]) = p_d \cdot \log[\max(D_{l\min}, D_l)/D_0] \quad \cdots \quad (7)$$

where D_l is the top depth to the layer whose S-wave velocity is l (in m/s) at the site, and p_d is a regression coef-

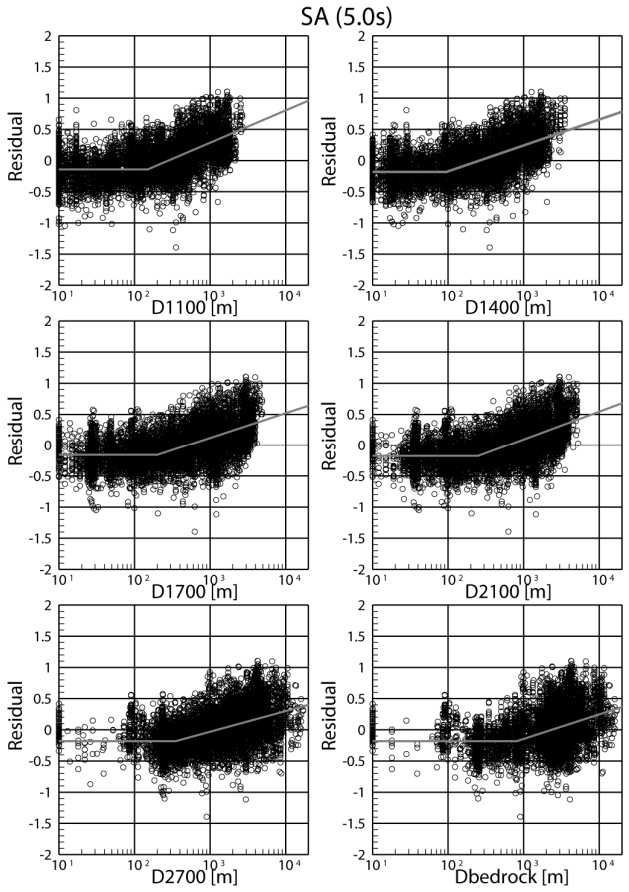

Fig. 4. Example of relation between residuals (log[obs/pre]) and depth to the layer whose S-wave velocity is l m/s (D_l). Gray lines are the obtained relations assuming the Eq. (7).

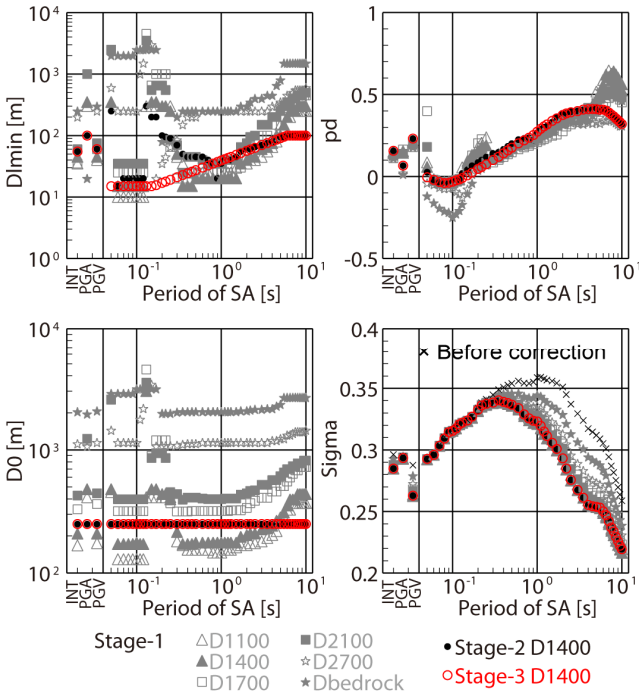

Fig. 5. Obtained coefficients of correction term for amplification by deep sediments.

ficient. We performed regression analysis in three stages:

(1) We obtained p_d changing $D_{l_{min}}$ and D_0 by 10 units for each D_l by trial and error. We selected D_{1400} as D_l because its standard deviation (sigma in **Fig. 5**) was the smallest of all strong-motion parameters from results.

(2) We fixed D_0 at 250 m as the average value for D_{1400} in stage 1 and obtained $D_{l_{min}}$ and p_d again (solid circle in **Fig. 5**).

(3) We smoothed coefficients $D_{l_{min}}$ and p_d to the period for the SA (open circle in **Fig. 5** and values in Appendix 1). Standard deviations before and after applying correction are also shown in **Fig. 5**. This correction is invalid for PGA and the SA at periods shorter than 0.3 s. The depth to the layer whose S-wave velocity is 1.0 km/s ($Z_{1.0}$) is used as a parameter in the NGA-west project in USA [19], and our results were generally consistent with those of that project.

4.2. Amplification by Shallow Soft Soils

The average S-wave velocity up to a 30 m depth ($Vs30$) at an observation station is a parameter useful for estimating amplification by shallow soft soils [20]. Based on a 7.5-arc-second engineering geomorphologic classification map, Matsuoka and Wakamatsu [21] constructed a $Vs30$ map that covered all of Japan, so we adopt the additional correction term corresponding to amplification by shallow soft soils using $Vs30$ as a parameter. $Vs30$ is defined as:

$$Vs30 = 30 / \sum_{l=1}^{nl} (H_l / Vs_l) \quad \ldots\ldots\ldots\ldots \quad (8)$$

where nl is the number of strata layers down to a depth of 30 m and H_l and Vs_l denote thickness (in m) and S-wave velocity (in m/s) of the l-th layer. To examine amplification by shallow soft soils, we extracted data from all data used in the above regression analysis using the following criteria:

(a) Focal depth is shallower than 30 km.

(b) Observed peak ground acceleration is smaller than 100 cm/s/s.

(c) The S-wave profile up to a 20 m depth is known.

In order to use many K-NET sites, we applied the relationship between $Vs30$ and average S-wave velocity up to a 20 m depth ($Vs20$ in m/s) [2]:

$$Vs30 = 1.13 Vs20 + 19.5 \quad \ldots\ldots\ldots\ldots \quad (9)$$

In order to avoid a double correction of site amplification, we adopted pre_{Gd} instead of pre in this section, which is the predicted amplitude calculated from the base model with correction by Eq. (7). **Fig. 6** shows an example of the relationship between the residual and $Vs30$.

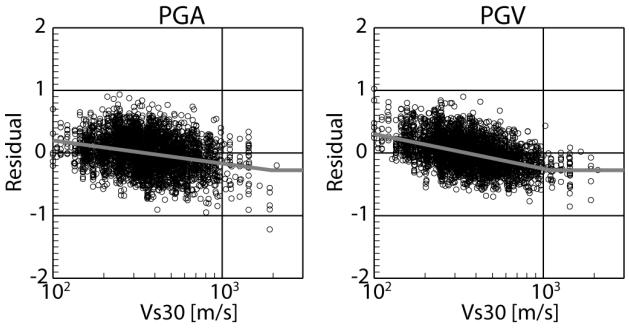

Fig. 6. Example of relation between residual ($\log[obs/pre_{Gd}]$) and average S-wave velocity up to 30 m depth ($Vs30$). Dashed lines are the obtained relations assuming the Eq. (10).

Note the trend of the residual becomes smaller so that $Vs30$ becomes larger. We modeled this trend as follows:

$$G_s(=\log[obs/pre_{Gd}]) = p_s \cdot \log[\min(Vs_{\max}, Vs30)/V_0] \quad \ldots (10)$$

where p_s is a regression coefficient. We performed regression analysis in three stages:

(1) We obtained V_0 and p_s changing Vs_{max} by 10 units (triangles in **Fig. 7**). Results showed that V_0 takes a value of about 350 m/s.

(2) We fixed V_0 at 350 m/s for all strong-motion parameters, and obtained Vs_{max} and p_s again (solid circles in **Fig. 7**).

(3) We smoothed coefficients Vs_{max} and p_s to the period for SA (open circles in **Fig. 7** and values in Appendix 1). Standard deviations before and after applying correction are shown in **Fig. 7**. Correction was most effective in a period of about 1 s. Correction was invalid, however, for SA at periods shorter than 0.1 s or longer than 5 s. When $Vs30$ is V_0, the value of the correction term becomes zero, so our base model obtained strong-motion amplitude at a relatively soft soil site whose $Vs30 = 350$ m/s.

This type of correction cannot, however, express the difference in the predominant period among a variety of site conditions, so this correction should be applied to obtain amplitude on engineering bedrock rather than on the ground surface.

4.3. Anomalous Seismic Intensity Distribution

The anomalous seismic intensity distribution seen during intermediate-depth and deep earthquakes is explained by a unique attenuation (Q) structure beneath the island-arc region as shown in **Fig. 8**. In order to express such a phenomenon, an additional correction term using the distance from a volcanic front to an observation site (X_{vf} in **Fig. 8**) as the parameter has been suggested [22]. The model is expressed as follows:

$$AI(=\log[obs/pre_G]) = \gamma \cdot X_{vf} \cdot (H-30) \quad \ldots (11)$$

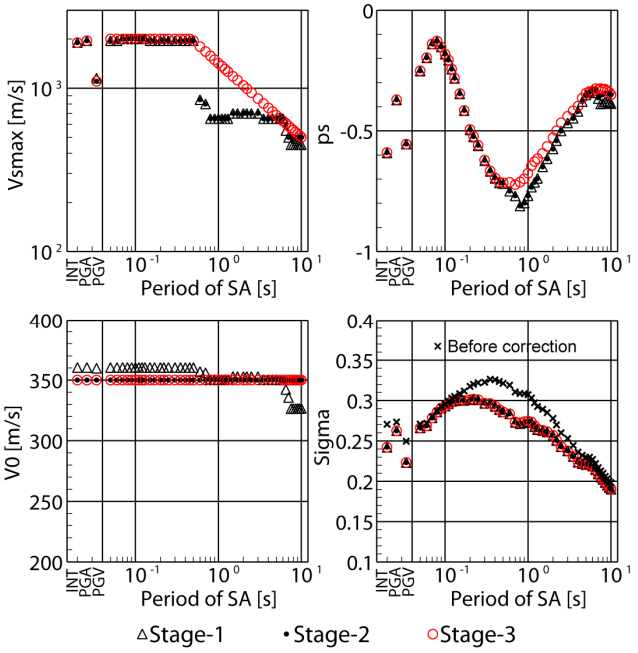

Fig. 7. Obtained coefficients of correction term for amplification by shallow soft soils.

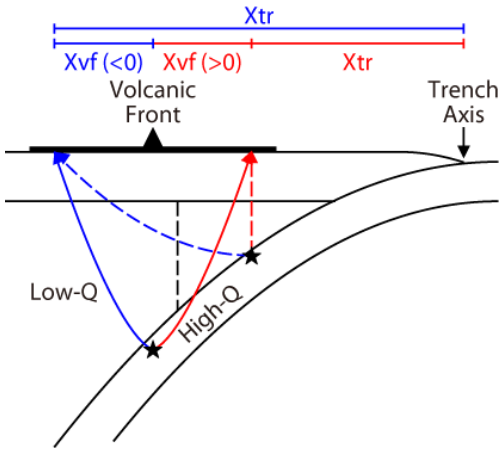

Fig. 8. Unique Q structure beneath island-arc region causing anomalous seismic intensity distribution [22].

where H is the focal depth of the earthquake (in km) and γ is the regression coefficient. In this section, we adopt pre_G instead of pre or pre_{Gd}, which is the predicted amplitude calculated from the base model with corrections by Eqs. (7) and (10). Note that this correction should only be applied to earthquakes whose focal depth is deeper than 30 km. To examine the anomalous seismic intensity distribution, we extracted data from all data used in the above regression analysis using the following criteria:

(a) The focal depth is deeper than 30 km.

(b) Observed peak ground acceleration is smaller than 100 cm/s/s.

The coefficient should be obtained for northeast Japan – earthquakes occurring at the Pacific Plate – and southwest

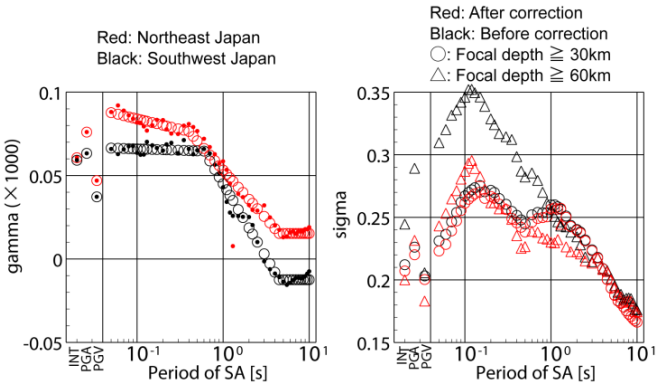

Fig. 9. Obtained coefficients for correction terms for anomalous seismic intensity distribution.

Japan – earthquakes occurring at the Philippine Sea Plate – individually. Based on past studies, we excluded strong-motion records observed at stations south of 36 degrees north in regression for northeast Japan because anomalous seismic intensity distribution is not seen [22], and we set the absolute value of X_{vf} to 75 km or less in the regression for southwest Japan [23]. Most strong-motion records obtained from shallow earthquakes whose focal depth was 40 km or less had an anomalous seismic intensity distribution that was not marked, so we perform regression analysis in three stages.

(1) We assumed the following model:

$$AI_i = \gamma_i \cdot X_{vf} \quad \ldots\ldots\ldots\ldots\ldots (12)$$

for each earthquake i and obtain γ_i for individual earthquakes.

(2) We assumed the following relationship:

$$\gamma_i = \gamma \cdot (H - 30) \quad \ldots\ldots\ldots\ldots\ldots (13)$$

and obtained γ (solid circles in **Fig. 9**). We adopted the following weights using the regression result of stage 1:

$$weight\_AI = \frac{N_i}{\sigma_{i\_AI}} \quad \ldots\ldots\ldots\ldots\ldots (14)$$

where N_i is the number of records for earthquake i. σ_i is the standard deviation for earthquake i obtained in stage 1.

(3) We performed smoothing for the period for SA (open circles in **Fig. 9** and values in Appendix 1). Standard deviations before and after applying correction was similar for all data. Note, however, that standard deviation after applying correction is very small when we limit data on earthquakes whose focal depth is deeper than 60 km only. This correction is invalid for SA at periods longer than 2 seconds. These results imply that Q-values for long period seismic waves are similar for fore-arc and back-arc region [24]. γ for northeast Japan is larger than that for southwest Japan. This means that the anomalous seismic intensity distribution is remarkable in northeast Japan.

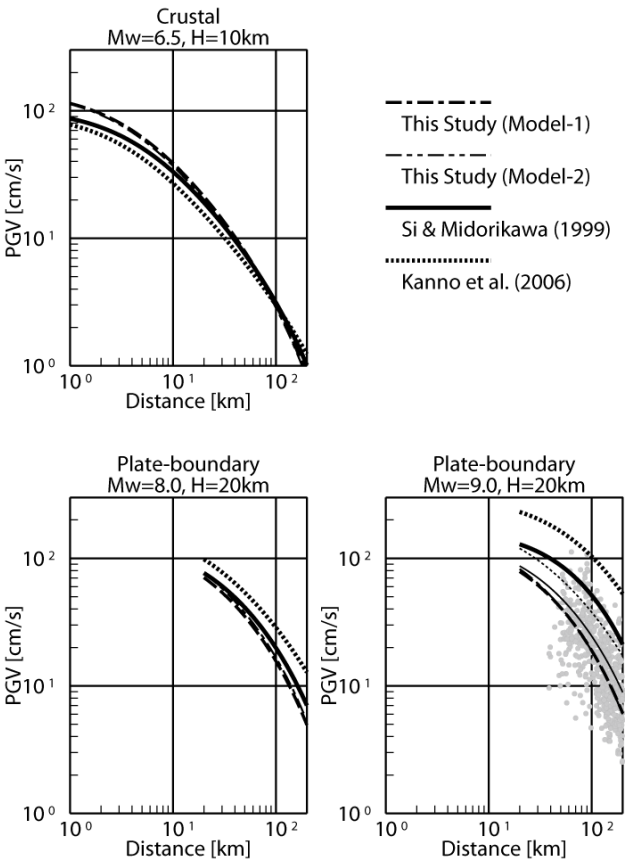

Fig. 10. Comparison of our new GMPE to existing Japanese GMPEs [1, 2] for PGV. H is the assumed focal depth required in the use of Si and Midorikawa's GMPE [1]. Thin lines in the right-lower panel are a case applying Mw = 8.2 instead of Mw = 9.0 for introducing magnitude saturation. Records observed during the 2011 earthquake are plotted using gray dots in the right-lower panel.

5. Discussion and Conclusions

Figure 10 compares our new GMPE to existing Japanese GMPEs [1, 2] for PGV. Site condition $Vs30$ is assumed to be 350 m/s and correction for amplification by deep sedimentary layers is not applied. PGV of Si and Midorikawa [1] is converted by using the relationship between $Vs30$ and the amplification factor of peak velocity [25]. PGV predicted by our new model is larger than that predicted by existing GMPEs for crustal earthquakes whose moment magnitude is 6.5. One reason may be that strong-motion records for very large amplitudes observed at near-source stations during the 2004 Niigata Chuetsu earthquake (Mw = 6.5) or the 2007 Iwate-Miyagi earthquake (Mw = 6.6) have been added to our database. Predicted PGV of about 100 km for which many strong-motion records are available is similar among GMPEs. In the case of subduction plate-boundary earthquakes with a moment magnitude of 8.0, PGV predicted by our new model is similar to that of Si and Midorikawa [1] in a near-source region. PGV predicted by our new model is much smaller, however, in the case of a moment magnitude of 9.0. This means that predicted PGV is greatly

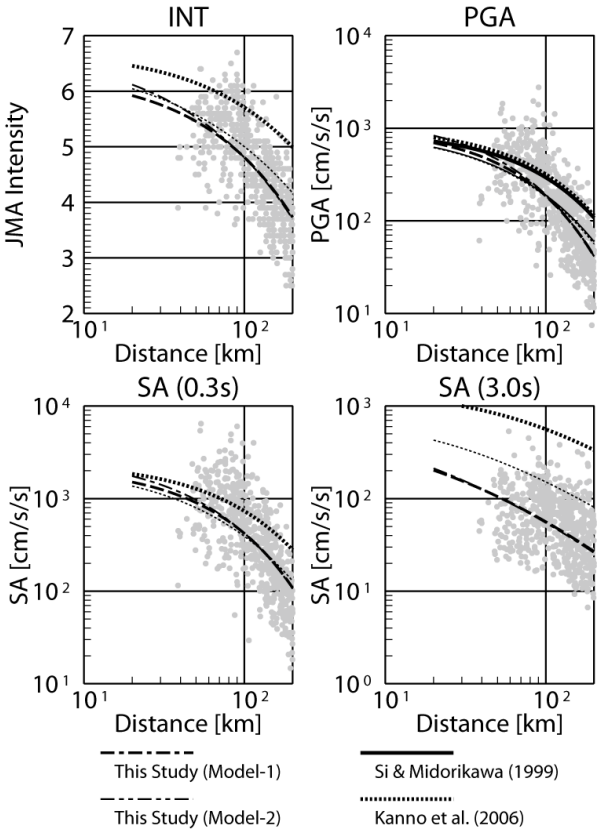

Fig. 11. Examples of comparison of our new GMPE to observed records during the 2011 earthquake (gray dots). Existing Japanese GMPE [2, 27] is also shown. Si and Midorikawa's GMPE [1] is also shown for PGA. Thin lines are a case applying Mw = 8.2 instead of Mw = 9.0 for introducing magnitude saturation.

overestimated when we apply Mw = 9.0 directly to existing Japanese GMPEs.

Using strong-motion records from the 2011 Tohoku-oki earthquake, we have identified a new GMPE applicable up to Mw9. Our target strong-motion parameters include the response spectrum for engineering use. **Fig. 11** shows examples comparing our new GMPE models with observed records from the 2011 Tohoku-oki earthquake. Our new models match observed records well for both PGV shown in **Fig. 10** and JMA seismic intensity, PGA and the acceleration response spectrum over a wide period range. Although existing Japanese GMPEs also match observed records in near-source region (<100 km) for PGA and a short SA period range when Mw = 9 is applied directly, these GMPEs clearly overestimate records at far sites. We examine two kinds of base models to express amplitude saturation at large magnitudes but could not determine which model was better. Both required amplitude saturation at Mw = 8.1 or 8.2 to explain observed strong-motion records during the 2011 Tohoku-oki earthquake, but the reason why amplitude saturates to magnitude is not clear. Some researchers pointed out that the amplitude did not saturate when the equivalent hypocenter distance was used as the source distance [26]. Research that solves this problem will be required in the future.

We adopted three additional correction terms that should be applied to base models to improve predictions. The correction term of the amplification by the deep sediments shown in this study was hardly taken into consideration in Japan until now, even though it is indispensable to long period ground motion to take this correction into consideration.

The evaluation of variation is very important in seismic hazard assessment. It is also necessary to consider both peak amplitude and the duration of ground motion for a mega-earthquake. We must study them much more to improve seismic hazard assessment in the future.

Acknowledgements

Strong-motion records used in this study were provided by the NIED, JMA, PARI, Central Research Institute of Electric Power Industry, Hanshin Expressway Public Corporation, Honshu-Shikoku Bridge Authority, Japan Railway Company Group, Kansai Electric Power Company, Kobe City Office, Konoike Construction, Co., Ltd., Kyoto University, Maeda Corporation, Matsumura-gumi Corporation, National Institute for Land and Infrastructure Management, Nippon Telegraph and Telephone Corporation, Obayashi Corporation, Osaka Gas Co., Ltd., Railway Technical Research Institute, Shiga Prefecture, Committee of Earthquake Observation and Research in Kansai Area, University of Shiga Prefecture, and Tokyo Electric Power Company, for which we thank all of these organizations. Prof. S. Midorikawa of the Tokyo Institute of Technology gave us valuable suggestions and comments on this study. Comments by the two reviewers greatly helped to improve this manuscript. This study was conducted as part of research on advanced seismic hazard assessment for national seismic hazard maps for Japan.

References:

[1] H. Si and S. Midoriakwa, "New attenuation relationships for peak ground acceleration and velocigy considering effects of fault type and site condition," Journal of Structural and Construction Engineering (Transactions of AIJ). Vol.523, pp. 63-70, 1999 (in Japanese with English abstract).

[2] T. Kanno, A. Narita, N. Morikawa, H. Fujiwara, and Y. Fukushima, "A new attenuation relation for strong ground motion in Japan based on recorded data," Bulletin of Seismological Society of America, Vol.96, pp. 879-897, 2006.

[3] Y. Yamanaka, "EIC seismological notes," 2004, http://www.eri.u-tokyo. ac.jp/sanchu/Seismo_Note/index-e.html [accessed April 15, 2013]

[4] K. Hikima and K. Koketsu, "Rupture processes of the 2004 Chuetsu (mid-Niigata prefecture) earthquake, Japan: a series of events in a complex fault system," Geophysical Research Letters, Vol.32, L18303, 2005.

[5] Geographical Survey Institute, "The mid Niigata prefecture earthquakes in 2004: Report index," 2004, http://cais.gis.go.jp/Research/topics/topic041023/topic_041023.html

[6] Subcommittee for Evaluation of Strong Ground Motion, Earthquake Research Committee, "On verification of the strong ground mottion evaluation method based on records of the 2005 west off Fukuoka earthquake," 2008 (in Japanese).

[7] S. Aoi and H. Sekiguchi, "Earthquakes during which K-NET and/or KiK-net observed JMA seismic intensity of 5+ or large," 2007 (in Japanese), http://www.kyoshin/bosai.go.jp/cgi-bin/kyoshin/bigeqs/index.cgi [accessed April 15, 2013]

[8] S. Aoi, H. Sekiguchi, N. Morikawa, and T. Kunugi, "Source process of the 2007 Niigata-ken Chuetsu-oki earthquake derived from near-fault strong motion data," Earth Planets Space, Vol.60, pp. 1131-1135, 2008.

[9] Y. Yamanaka, "NGY seismological notes," 2008 (in Japanese), http://www.seis.nagoya-u.ac.jp/sanchu/Seismo_Note [accessed April 15, 2013]

[10] W. Suzuki, S. Aoi, and H. Sekiguchi, "Rupture process of the 2008 Iwate-Miyagi Nairiku, Japan, earthquake derived from near-source strong motion records," Bulletin of Seismological Society of America, Vol.100, pp. 256-266, 2010.

[11] W. Suzuki, S. Aoi, and H. Sekiguchi, "Rupture process of the 2008 northern Iwate intraslab earthquake derived from strong-motion records, Bulletin of Seismological Society of America, Vol.99, pp. 2825-2835, 2009.

[12] S. Aoi, B. Enescu, W. Suzuki, Y. Asano, K. Obara, T. Kunugi, and K. Shiomi, "Stress transfer in the Tokai subduction zone from the 2009 Suruga bay earthquake in Japan," Nature Geoscience, Vol.3, doi:10.1038/NGEO885, 2010.

[13] Japan Meteorological Agency, "Results of source process analysis of remarkable earthquake occurred in and around Japan," 2011 (in Japanese), http://www.seisvol.kishou.go.jp/eq/sourceprocess/index.html [accessed April 15, 2013]

[14] Earthquake Research Committee, "evaluation of the 2011 Tohoku-oki earthquake," 2011 (in Japanese).

[15] Y. Fukushima, "Scaling relations for strong ground motion prediction models with M2 terms," Bulletin of the Seicmological Society of America, Vol.86, pp. 329-336, 1996.

[16] Y. Fukushima and T. Tanaka, "A new attenuation relation for peak horizontal acceleration of strong motion in Japan," Bulletin of Seismological Society of America, Vol.86, pp. 329-336, 1990.

[17] Y. Fukushima, C. Berge-Thierry, P. Volant, D. A. Griot-Pommera, and F. Cotton, "Attenuation relation for West Eurasia determined with recent near-fault records from Clifornia, Japan and Turkey," Journal of Earthquake Engineering, Vol.7, No.3, pp. 1-26, 2003.

[18] H. Fujiwara, S. Kawai, S. Aoi, N. Morikawa, S. Senna, N. Kudo, M. Ooi, K.-X. Hao, Y. Hayakawa, N. Toyama, H. Matsuyama, K. Iwamoto, H. Suzuki, and E. Ryu, "A strudy on subsurface structure model for deep sedimentary layers of Japan for strong-motion evaluation," Technical Note of the National Research Institute for Earch Science and Disaster Prevention, No.337, 2009 (in Japanese).

[19] D. M. Boore and G. M. Atkinson, "Ground-motion prediction equations for the average horizontal component of PGA, PGV, and 5%-damped PSA at spectral periods between 0.01 s and 10.0 s," Earthquake Spectra, Vol.24, pp. 99-138, 2008.

[20] W. B. Joyner and T. E. Fumal, "Use of measured shear-wave velocity for predicting geologic site effects on strong ground motion," Proceedings of 8th World Conference on Earthquake Engineering, Vol.2, pp. 777-783, 1984.

[21] M. Matsuoka and K. Wakamatsu, "Site amplification capability map based on the 7.5-arc-second Japan engineering geomorphologic classification map," National Institute of Advanced Industrial Science and Technology, Intellectural property management, No.H20PRO-936, 2008.

[22] N. Morikawa, T. Kanno, A. Narita, H. Fujiwara, and Y. Fukushima, "Additional Correction Terms for Attenuation Relations of Peak Amplitdes and Response Spectra Corresponding to the Anomalous Seismic Intensity in Northeastern Japan," Journal of Japan Earthquake Engineering Society, Vol.6, No.1, pp. 23-41, 2006 (in Japanese with English abstract).

[23] N. Morikawa, T. Kanno, A. Narita, H. Fujiwara, and Y. Fukushima, "Additional correction terms for atteunation relations correspoinding to the anomalous seismic intensity in southwest Japan,," Programme and Abstracts of Seismological Society of Japan, 2006.

[24] T. Maeda and T. Sasatani, "Effects of the anomalous upper mantle structure on strong ground motion," Geophysical Bulletin of Hokkaido Unversity, No.64, pp. 91-113, 2001 (in Japanese with English abstract).

[25] K. Fujimoto and S. Midorikawa, "Relationship between average shear-wave velocity and site amplification inferred from storong motion records at nearby station pairs," Journal of Japan Association for Earthquake Engineering, Vol.6, No.1, pp. 11-22, 2006 (in Japanese with English abstract).

[26] S. Ohno, "Strong-motion observation records during the 2011 Tohoku earthquake," The 39th Symposium of Earthquake Ground Motion (2011), pp. 13-20, 2011 (in Japanese with English abstract).

[27] N. Morikawa, T. Kanno, A. Narita, H. Fujiwara, and Y. Fukushima "A New Attenuation Relation of Seismic Intensity for Japan Based on Recent Strong-Motion Records," Geophyisical Bulletin of Hokkaido University, No.73, pp. 149-158, 2010 (in Japanese).

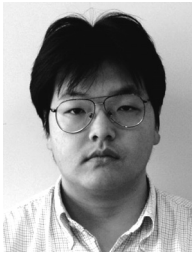

Name:
Nobuyuki Morikawa

Affiliation:
Senior Researcher, National Research Institute for Earth Science and Disaster Prevention

Address:
Tennodai 3-1, Tsukuba-shi, Ibaraki 305-0006, Japan

Brief Career:
2001- National Research Institute for Earth Science and Disaster Prevention

Academic Societies & Scientific Organizations:
- Seismological Society of Japan (SSJ)
- Japan Association for Earthquake Engineering (JAEE)

Name:
Hiroyuki Fujiwara

Affiliation:
Director, Department of Integrated Research on Disaster Prevention, National Research Institute for Earth Science and Disaster Prevention

Address:
3-1 Tennodai, Tsukuba, Ibaraki 305-0006, Japan

Brief Career:
1989- Researcher, NIED
2001- Head of strong motion observation network laboratory, NIED
2006- Project director, Disaster prevention system research center, NIED
2011- Director, Social system research department, NIED

Academic Societies & Scientific Organizations:
- Seismological Society of Japan (SSJ)
- Japan Association for Earthquake Engineering (JAEE)

Appendix A.

Table 2. Model 1.

Parameter		M_{w01}	M_{w1}	a_1	b_{1_I}	b_{1_II}	b_{1_III}	c_{1_I}	c_{1_II}	c_{1_III}	d_1	e_1	σ_1
INT		8.2	16.0	-0.0321	-0.003736	-0.003320	-0.004195	6.9301	6.9042	7.2975	0.005078	0.5	0.3493
PGA		8.2	16.0	-0.0321	-0.005315	-0.005042	-0.005605	7.0830	7.1181	7.5035	0.011641	0.5	0.3761
PGV		8.2	16.0	-0.0325	-0.002654	-0.002408	-0.003451	5.6952	5.6026	6.0030	0.002266	0.5	0.3399
5% damped acceleration spectrum (SA)	0.05s	8.2	16.0	-0.0321	-0.005912	-0.005674	-0.006231	7.2151	7.2759	7.6801	0.012812	0.5	0.3938
	0.06s	8.2	16.0	-0.0321	-0.006097	-0.005864	-0.006405	7.2852	7.3523	7.7504	0.014508	0.5	0.4039
	0.07s	8.2	16.0	-0.0321	-0.006142	-0.005967	-0.006507	7.3397	7.4152	7.8127	0.015574	0.5	0.4149
	0.08s	8.2	16.0	-0.0323	-0.006104	-0.006033	-0.006594	7.4122	7.4929	7.8938	0.016465	0.5	0.4219
	0.09s	8.2	16.0	-0.0325	-0.006112	-0.006079	-0.006689	7.4817	7.5649	7.9649	0.017390	0.5	0.4259
	0.10s	8.2	16.0	-0.0327	-0.006116	-0.006061	-0.006686	7.5396	7.6214	8.0219	0.018438	0.5	0.4266
	0.11s	8.2	16.0	-0.0324	-0.005998	-0.005971	-0.006576	7.5072	7.5947	7.9960	0.017396	0.5	0.4256
	0.12s	8.2	16.0	-0.0322	-0.005896	-0.005878	-0.006448	7.4920	7.5837	7.9782	0.016457	0.5	0.4243
	0.13s	8.2	16.0	-0.0321	-0.005786	-0.005757	-0.006331	7.4788	7.5645	7.9644	0.015607	0.5	0.4229
	0.15s	8.2	16.0	-0.0321	-0.005564	-0.005579	-0.006078	7.4630	7.5471	7.9360	0.014118	0.5	0.4193
	0.17s	8.2	16.0	-0.0321	-0.005398	-0.005382	-0.005813	7.4557	7.5245	7.9097	0.012855	0.5	0.4162
	0.20s	8.2	16.0	-0.0321	-0.005151	-0.005027	-0.005476	7.4307	7.4788	7.8719	0.011273	0.5	0.4152
	0.22s	8.2	16.0	-0.0322	-0.005000	-0.004827	-0.005204	7.4139	7.4461	7.8311	0.010380	0.5	0.4130
	0.25s	8.2	16.0	-0.0321	-0.004836	-0.004519	-0.004907	7.3736	7.3728	7.7521	0.009225	0.5	0.4089
	0.30s	8.2	16.0	-0.0321	-0.004543	-0.004095	-0.004621	7.2924	7.2797	7.6656	0.007670	0.5	0.4063
	0.35s	8.2	16.0	-0.0321	-0.004379	-0.003717	-0.004305	7.2417	7.1832	7.5796	0.006448	0.5	0.4043
	0.40s	8.2	16.0	-0.0321	-0.004135	-0.003342	-0.003989	7.1785	7.0883	7.4889	0.005464	0.5	0.4029
	0.45s	8.2	16.0	-0.0321	-0.003973	-0.003063	-0.003934	7.1202	7.0100	7.4287	0.004657	0.5	0.4033
	0.50s	8.2	16.0	-0.0321	-0.003767	-0.002832	-0.003783	7.0604	6.9439	7.3615	0.003986	0.5	0.4019
	0.60s	8.2	16.0	-0.0321	-0.003389	-0.002450	-0.003351	6.9357	6.8166	7.2161	0.002946	0.5	0.4032
	0.70s	8.2	16.0	-0.0321	-0.002981	-0.002059	-0.002988	6.8272	6.6957	7.0854	0.002193	0.5	0.4038
	0.80s	8.2	16.0	-0.0321	-0.002640	-0.001692	-0.002587	6.7325	6.5864	6.9659	0.001641	0.5	0.4053
	0.90s	8.2	16.0	-0.0325	-0.002341	-0.001445	-0.002421	6.6845	6.5349	6.9211	0.001234	0.5	0.4085
	1.0s	8.2	16.0	-0.0327	-0.002138	-0.001322	-0.002331	6.6284	6.4748	6.8605	0.000936	0.5	0.4091
	1.1s	8.2	16.0	-0.0331	-0.001912	-0.001140	-0.002194	6.5971	6.4383	6.8304	0.000723	0.5	0.4074
	1.2s	8.2	16.0	-0.0337	-0.001790	-0.001053	-0.002213	6.5912	6.4200	6.8224	0.000576	0.5	0.4061
	1.3s	8.2	16.0	-0.0339	-0.001671	-0.000979	-0.002159	6.5588	6.3848	6.7827	0.000482	0.5	0.4046
	1.5s	8.2	16.0	-0.0347	-0.001516	-0.000811	-0.002020	6.5419	6.3510	6.7540	0.000417	0.5	0.4035
	1.7s	8.2	16.0	-0.0352	-0.001526	-0.000714	-0.001909	6.5209	6.3011	6.7004	0.000471	0.5	0.4007
	2.0s	8.2	16.0	-0.0359	-0.001604	-0.000673	-0.001576	6.4982	6.2617	6.6087	0.000703	0.5	0.3927
	2.2s	8.2	16.0	-0.0365	-0.001516	-0.000610	-0.001349	6.4920	6.2463	6.5766	0.000702	0.5	0.3883
	2.5s	8.2	16.0	-0.0375	-0.001457	-0.000586	-0.001266	6.4964	6.2485	6.5667	0.000826	0.5	0.3831
	3.0s	8.2	16.0	-0.0382	-0.001345	-0.000505	-0.001105	6.4414	6.1858	6.4858	0.001202	0.5	0.3775
	3.5s	8.2	16.0	-0.0384	-0.001270	-0.000512	-0.001000	6.3464	6.0849	6.3681	0.001647	0.5	0.3713
	4.0s	8.2	16.0	-0.0385	-0.001075	-0.000610	-0.001005	6.2459	6.0035	6.2727	0.002087	0.5	0.3646
	4.5s	8.2	16.0	-0.0389	-0.000904	-0.000605	-0.001061	6.1868	5.9423	6.2145	0.002489	0.5	0.3603
	5.0s	8.2	16.0	-0.0393	-0.000739	-0.000564	-0.001155	6.1466	5.8960	6.1817	0.002841	0.5	0.3552
	5.5s	8.2	16.0	-0.0398	-0.000570	-0.000626	-0.001254	6.1084	5.8725	6.1566	0.003139	0.5	0.3494
	6.0s	8.2	16.0	-0.0402	-0.000456	-0.000702	-0.001317	6.0920	5.8536	6.1257	0.003384	0.5	0.3428
	6.5s	8.2	16.0	-0.0405	-0.000308	-0.000785	-0.001361	6.0636	5.8218	6.0778	0.003580	0.5	0.3366
	7.0s	8.2	16.0	-0.041	-0.000195	-0.000856	-0.001392	6.0586	5.8197	6.0652	0.003728	0.5	0.3300
	7.5s	8.2	16.0	-0.0412	-0.000109	-0.000880	-0.001413	6.0367	5.7971	6.0388	0.003833	0.5	0.3242
	8.0s	8.2	16.0	-0.0417	-0.000100	-0.000908	-0.001466	6.0378	5.7885	6.0381	0.003898	0.5	0.3185
	8.5s	8.2	16.0	-0.0419	-0.000100	-0.000940	-0.001496	6.0238	5.7674	6.0180	0.003927	0.5	0.3130
	9.0s	8.2	16.0	-0.042	-0.000100	-0.001012	-0.001488	5.9972	5.7463	5.9881	0.003924	0.5	0.3090
	9.5s	8.2	16.0	-0.0423	-0.000100	-0.001098	-0.001485	5.9880	5.7507	5.9807	0.003890	0.5	0.3047
	10.0s	8.2	16.0	-0.0427	-0.000100	-0.001179	-0.001498	5.9820	5.7595	5.9869	0.003828	0.5	0.3007

Table 3. Model 2.

Parameter		Mw_{02}	a_2	b_{2_I}	b_{2_II}	b_{2_III}	c_{2_I}	c_{2_II}	c_{2_III}	d_2	e_2	σ_2
INT		8.1	0.5583	-0.0031	-0.003064	-0.003986	0.2929	0.3032	0.7083	0.002734	0.5	0.350557
PGA		8.1	0.5507	-0.004531	-0.004716	-0.005273	0.4631	0.5418	0.9338	0.006875	0.5	0.377556
PGV		8.1	0.6014	-0.002602	-0.002375	-0.003435	-1.1779	-1.2682	-0.8601	0.002109	0.5	0.341184
5% damped acceleration spectrum (SA)	0.05s	8.1	0.5568	-0.005262	-0.005398	-0.005944	0.5742	0.6708	1.0802	0.008437	0.5	0.39585
	0.06s	8.1	0.5583	-0.005486	-0.005602	-0.006124	0.6363	0.7372	1.1392	0.009935	0.5	0.406216
	0.07s	8.1	0.567	-0.005727	-0.005783	-0.006308	0.6664	0.7641	1.1651	0.012141	0.5	0.417324
	0.08s	8.1	0.581	-0.00584	-0.005908	-0.006463	0.6513	0.7448	1.1503	0.014089	0.5	0.424299
	0.09s	8.1	0.5882	-0.005904	-0.005977	-0.006584	0.6627	0.7553	1.16	0.015398	0.5	0.428249
	0.10s	8.1	0.59	-0.005864	-0.005942	-0.006557	0.6796	0.7734	1.1781	0.015938	0.5	0.428989
	0.11s	8.1	0.5816	-0.005714	-0.005838	-0.006434	0.7294	0.831	1.2364	0.014729	0.5	0.427985
	0.12s	8.1	0.5773	-0.005582	-0.005734	-0.006294	0.751	0.8585	1.2571	0.013673	0.5	0.426643
	0.13s	8.1	0.5741	-0.005447	-0.005602	-0.006167	0.7651	0.8681	1.2724	0.012742	0.5	0.425182
	0.15s	8.1	0.5672	-0.005182	-0.005408	-0.005899	0.7951	0.9	1.2926	0.011173	0.5	0.421309
	0.17s	8.1	0.566	-0.004982	-0.005198	-0.005624	0.7913	0.8827	1.2723	0.009898	0.5	0.417951
	0.20s	8.1	0.5692	-0.004697	-0.004829	-0.005279	0.7354	0.8075	1.2069	0.008375	0.5	0.416664
	0.22s	8.1	0.5696	-0.004527	-0.004623	-0.005005	0.7099	0.7672	1.1591	0.00755	0.5	0.414311
	0.25s	8.1	0.5666	-0.004343	-0.004309	-0.004708	0.6973	0.7227	1.1097	0.006522	0.5	0.409973
	0.30s	8.1	0.563	-0.004033	-0.00388	-0.004427	0.639	0.6544	1.0482	0.005205	0.5	0.407229
	0.35s	8.1	0.5631	-0.003866	-0.003504	-0.004121	0.589	0.559	0.9643	0.004226	0.5	0.40497
	0.40s	8.1	0.5603	-0.00363	-0.003134	-0.003817	0.5465	0.4852	0.8946	0.003474	0.5	0.40347
	0.45s	8.1	0.5656	-0.003482	-0.002863	-0.003775	0.4569	0.3742	0.8033	0.002883	0.5	0.403898
	0.50s	8.1	0.5718	-0.003297	-0.002642	-0.003637	0.3608	0.2699	0.6996	0.002411	0.5	0.402479
	0.60s	8.1	0.5723	-0.00297	-0.002285	-0.003231	0.2414	0.1461	0.5569	0.001717	0.5	0.403992
	0.70s	8.1	0.5743	-0.002622	-0.001921	-0.002893	0.1288	0.0186	0.4186	0.001246	0.5	0.404778
	0.80s	8.1	0.5829	-0.002342	-0.00158	-0.002513	-0.013	-0.1418	0.2487	0.000923	0.5	0.406362
	0.90s	8.1	0.5952	-0.002102	-0.001357	-0.002365	-0.1727	-0.3082	0.0883	0.0007	0.5	0.40959
	1.0s	8.1	0.6011	-0.001955	-0.001256	-0.00229	-0.2766	-0.4191	-0.024	0.00055	0.5	0.410513
	1.1s	8.1	0.6116	-0.001777	-0.001092	-0.002165	-0.4106	-0.5607	-0.1601	0.000453	0.5	0.408831
	1.2s	8.1	0.6235	-0.001697	-0.001019	-0.002193	-0.5377	-0.7024	-0.2922	0.000395	0.5	0.407583
	1.3s	8.1	0.6299	-0.001611	-0.000956	-0.002146	-0.6329	-0.8022	-0.3972	0.000368	0.5	0.406247
	1.5s	8.1	0.6465	-0.001495	-0.000801	-0.002016	-0.826	-1.0147	-0.6049	0.000379	0.5	0.405023
	1.7s	8.1	0.6562	-0.001515	-0.000707	-0.001906	-0.9542	-1.1723	-0.7663	0.00045	0.5	0.402318
	2.0s	8.1	0.668	-0.001566	-0.000655	-0.001567	-1.1204	-1.354	-0.9994	0.000625	0.5	0.394334
	2.2s	8.1	0.6793	-0.001473	-0.000591	-0.001339	-1.2569	-1.4994	-1.1613	0.000613	0.5	0.389792
	2.5s	8.1	0.6961	-0.001401	-0.000562	-0.001253	-1.4482	-1.6922	-1.3657	0.000708	0.5	0.384315
	3.0s	8.1	0.7089	-0.001267	-0.00047	-0.001086	-1.6579	-1.9088	-1.5998	0.001021	0.5	0.379064
	3.5s	8.1	0.7108	-0.001176	-0.000469	-0.000976	-1.783	-2.0392	-1.7466	0.001407	0.5	0.373438
	4.0s	8.1	0.7126	-0.00097	-0.000561	-0.000977	-1.9099	-2.1469	-1.8681	0.0018	0.5	0.367629
	4.5s	8.1	0.7188	-0.000796	-0.000552	-0.00103	-2.0423	-2.2814	-1.9993	0.00217	0.5	0.363713
	5.0s	8.1	0.727	-0.000631	-0.00051	-0.001123	-2.1763	-2.4219	-2.1263	0.002505	0.5	0.358918
	5.5s	8.1	0.7347	-0.000466	-0.000573	-0.001222	-2.3029	-2.5338	-2.2399	0.0028	0.5	0.353314
	6.0s	8.1	0.743	-0.000359	-0.000651	-0.001286	-2.4133	-2.647	-2.3651	0.003055	0.5	0.346944
	6.5s	8.1	0.7481	-0.000219	-0.000736	-0.001333	-2.496	-2.7338	-2.4684	0.003272	0.5	0.340642
	7.0s	8.1	0.7576	-0.000118	-0.000811	-0.001367	-2.6064	-2.8423	-2.5873	0.003452	0.5	0.333811
	7.5s	8.1	0.7637	-0.0001	-0.00084	-0.001391	-2.693	-2.93	-2.6791	0.003598	0.5	0.328188
	8.0s	8.1	0.7722	-0.0001	-0.000873	-0.001449	-2.7828	-3.0304	-2.7717	0.003713	0.5	0.322025
	8.5s	8.1	0.7769	-0.0001	-0.000911	-0.001485	-2.8447	-3.1003	-2.8406	0.003799	0.5	0.315922
	9.0s	8.1	0.7798	-0.0001	-0.00099	-0.001482	-2.8983	-3.1492	-2.8983	0.003858	0.5	0.311422
	9.5s	8.1	0.787	-0.0001	-0.001083	-0.001485	-2.9822	-3.2205	-2.9816	0.003893	0.5	0.306796
	10.0s	8.1	0.7954	-0.000115	-0.001171	-0.001505	-3.077	-3.3014	-3.0654	0.003906	0.5	0.302647

Table 4. Additional correction terms.

Parameter		p_d	D_{lmin}	D_0	p_s	Vs_{max}	V_0	$\gamma\_NEJapan$	$\gamma\_SWJapan$
INT		0.1575	55.00	250	-0.5898	1900.00	350	0.00006066	0.00005914
PGA		0.0663	100.00	250	-0.3709	1950.00	350	0.00007602	0.00006327
PGV		0.2317	60.00	250	-0.5546	1100.00	350	0.00004693	0.00003721
5% damped acceleration spectrum (SA)	0.05s	-0.0043	15.00	250	-0.2513	2000.00	350	0.00008768	0.00006642
	0.06s	-0.0205	15.00	250	-0.1966	2000.00	350	0.00008669	0.00006629
	0.07s	-0.0335	15.00	250	-0.1393	2000.00	350	0.00008585	0.00006618
	0.08s	-0.0396	15.00	250	-0.1279	2000.00	350	0.00008512	0.00006608
	0.09s	-0.0383	15.00	250	-0.1517	2000.00	350	0.00008449	0.00006599
	0.10s	-0.0315	15.00	250	-0.1819	2000.00	350	0.00008391	0.00006592
	0.11s	-0.0236	15.00	250	-0.2067	2000.00	350	0.00008340	0.00006585
	0.12s	-0.0176	15.00	250	-0.2436	2000.00	350	0.00008292	0.00006578
	0.13s	-0.0088	15.00	250	-0.2815	2000.00	350	0.00008249	0.00006572
	0.15s	0.0072	15.00	250	-0.3454	2000.00	350	0.00008171	0.00006562
	0.17s	0.0235	15.62	250	-0.4150	2000.00	350	0.00008103	0.00006553
	0.20s	0.0460	17.00	250	-0.4943	2000.00	350	0.00008015	0.00006541
	0.22s	0.0583	17.86	250	-0.5235	2000.00	350	0.00007963	0.00006534
	0.25s	0.0746	19.09	250	-0.5598	2000.00	350	0.00007894	0.00006525
	0.30s	0.1006	21.00	250	-0.6217	2000.00	350	0.00007711	0.00006511
	0.35s	0.1206	22.75	250	-0.6654	2000.00	350	0.00007639	0.00006500
	0.40s	0.1418	24.39	250	-0.6945	2000.00	350	0.00007341	0.00006491
	0.45s	0.1599	25.93	250	-0.7129	2000.00	350	0.00007075	0.00006482
	0.50s	0.1760	27.40	250	-0.7160	1950.00	350	0.00006614	0.00006474
	0.60s	0.2023	30.13	250	-0.7134	1794.99	350	0.00008249	0.00006461
	0.70s	0.2207	32.65	250	-0.7224	1673.59	350	0.00006225	0.00005872
	0.80s	0.2370	35.00	250	-0.7116	1575.08	350	0.00005888	0.00005361
	0.90s	0.2532	37.22	250	-0.6982	1493.01	350	0.00005590	0.00004911
	1.0s	0.2744	39.32	250	-0.6755	1423.23	350	0.00005324	0.00004508
	1.1s	0.2917	41.32	250	-0.6447	1362.92	350	0.00005083	0.00004143
	1.2s	0.3062	43.23	250	-0.6270	1310.09	350	0.00004863	0.00003811
	1.3s	0.3175	45.07	250	-0.6156	1263.31	350	0.00004661	0.00003504
	1.5s	0.3391	48.56	250	-0.5929	1183.79	350	0.00004299	0.00002957
	1.7s	0.3552	51.84	250	-0.5648	1118.36	350	0.00003983	0.00002489
	2.0s	0.3759	56.42	250	-0.5283	1038.76	350	0.00003573	0.00001857
	2.2s	0.3846	59.29	250	-0.4995	994.74	350	0.00003332	0.00001493
	2.5s	0.3916	63.37	250	-0.4661	938.62	350	0.00003009	0.00001004
	3.0s	0.3996	69.69	250	-0.4398	864.01	350	0.00002548	0.00000307
	3.5s	0.4085	75.52	250	-0.4168	805.57	350	0.00002159	-0.00000283
	4.0s	0.4108	80.96	250	-0.3976	758.15	350	0.00001821	-0.00000793
	4.5s	0.4120	86.08	250	-0.3653	718.65	350	0.00001524	-0.00000124
	5.0s	0.4109	90.94	250	-0.3443	685.06	350	0.00001524	-0.00000124
	5.5s	0.4078	95.57	250	-0.3370	656.03	350	0.00001524	-0.00000124
	6.0s	0.4088	100.00	250	-0.3374	630.60	350	0.00001524	-0.00000124
	6.5s	0.4020	100.00	250	-0.3251	608.09	350	0.00001524	-0.00000124
	7.0s	0.3910	100.00	250	-0.3294	587.95	350	0.00001524	-0.00000124
	7.5s	0.3783	100.00	250	-0.3252	569.81	350	0.00001524	-0.00000124
	8.0s	0.3671	100.00	250	-0.3267	553.35	350	0.00001524	-0.00000124
	8.5s	0.3553	100.00	250	-0.3271	538.31	350	0.00001524	-0.00000124
	9.0s	0.3438	100.00	250	-0.3332	524.51	350	0.00001524	-0.00000124
	9.5s	0.3320	100.00	250	-0.3409	511.79	350	0.00001524	-0.00000124
	10.0s	0.3202	100.00	250	-0.3501	500.00	350	0.00001524	-0.00000124